1 **RESEARCH PAPER**

2

3 **KAKU4-mediated deformation of the vegetative nucleus controls its**

4 **precedent migration over sperm cells in pollen tubes**

5

6 Chieko Goto[1,2,3], Kentaro Tamura[1,4*], Satsuki Nishimaki[5], Naoki Yanagisawa[6], Kumi

7 Matsuura-Tokita[6], Tetsuya Higashiyama[6], Daisuke Maruyama[5], and Ikuko

8 Hara-Nishimura[1,7*]

9

10 [1] Graduate School of Science, Kyoto University, Kyoto 606-8502, Japan.

11 [2] Graduate School of Agricultural and Life Sciences, The University of Tokyo, Tokyo

12 113-8657, Japan.

13 [3]Institut de biologie moléculaire des plantes, CNRS, Université de Strasbourg, 67000

14 Strasbourg, France.

15 [4] School of Food and Nutritional Sciences, University of Shizuoka, Shizuoka 422-8526,

16 Japan.

17 [5] Kihara Institute for Biological Research, Yokohama City University, Yokohama

18 244-0813, Japan.

19 [6] Institute of Transformative Bio Molecules, Nagoya University, Nagoya 464-8601,

20 Japan.

21 [7] Faculty of Science and Engineering, Konan University, Kobe 658-8501, Japan.

22

23 *Correspondence: Ikuko Hara-Nishimura< ihnishi@gr.bot.kyoto-u.ac.jp>

24 and Kentaro Tamura <tamura@u-shizuoka-ken.ac.jp>

25

26 The date of submission: 8 September 2019

27 One table, seven figures, and two supplemental figures.

28 Word count: 3,967 words

29

30 **Running title**: KAKU4 controls migration of the nucleus in pollen tubes

Highlight

The nuclear envelope protein KAKU4 is involved in controlling the migration order of vegetative nuclei and sperm cells in pollen tubes, affecting the competitive ability of pollen for fertilization.

Abstract

A putative nuclear lamina protein, KAKU4, modulates nuclear morphology in *Arabidopsis thaliana* seedlings but its physiological significance is unknown. *KAKU4* was strongly expressed in mature pollen grains, each of which has a vegetative cell and two sperm cells. KAKU4 protein was highly abundant on the envelopes of vegetative nuclei (VNs) and less abundant on the envelopes of sperm cell nuclei (SCNs) in pollen grains and elongating pollen tubes. VN is irregularly shaped in wild-type pollen. However, *KAKU4* deficiency caused it to become more spherical. These results suggest that the dense accumulation of KAKU4 is responsible for the irregular shape of the VNs. After a pollen grain germinates, the VN and SCNs migrate to the tip of the pollen tube. In the wild type, the VN preceded the SCNs in 91–93% of the pollen tubes, whereas in *kaku4* mutants, the VN trailed the SCNs in 39–58% of the pollen tubes. *kaku4* pollen was less competitive than wild-type pollen after pollination, although it had an ability to fertilize. Taken together, our results suggest that controlling the nuclear shape in vegetative cells of pollen grains by *KAKU4* ensures the orderly migration of the VN and sperm cells in pollen tubes.

Key words: *Arabidopsis thaliana*, fertilization, KAKU4, male germ unit, nuclear envelope, nuclear shape, nuclear lamina, pollen tube, vegetative nucleus, sperm cells.

Abbreviations: CRWN, CROWDED NUCLEI; SCN, sperm cell nucleus; SUN, Sad1/UNC84 Homology; VN, vegetative nucleus; WIP, WPP domain–interacting protein; WIT, WPP domain–interacting tail-anchored protein.

Introduction

In *Arabidopsis thaliana*, pollen grains contain a vegetative cell and two sperm cells (Borg and Twell, 2011; McCue *et al.*, 2011). One of the sperm cells fertilizes the egg cell to produce the embryo and the other fertilizes the central cell to produce the endosperm (Hamamura *et al.*, 2011; Kawashima and Berger, 2011; Maruyama *et al.*, 2015). The vegetative nucleus (VN) has irregular shapes (Vogler *et al.*, 2015) and is physically connected to one of the two sperm cells. Together, the VN and the two sperm cells form a functional unit termed the male germ unit (McCue *et al.,* 2011). After pollination, the pollen grain germinates. Then, the VN and its trailing sperm cells move into and migrate along the elongating pollen tube, although they occasionally change their migration order (Zhou and Meier, 2014).

Nuclear movements are driven by the plant-specific motor protein myosin XI-i (Tamura *et al.*, 2013). In *A. thaliana*, the migration order of the VN and sperm cells is not affected by myosin XI-I deficiency (Zhou and Meier, 2014), but it is affected by the outer nuclear membrane proteins WIPs (WIP1, WIP2, and WIP3) and WITs (WIT1 and WIT2) and the possible inner nuclear membrane proteins SUNs (SUN1 and SUN2) (Zhou *et al.*, 2015; Zhou and Meier, 2014).

Plant nuclei have a fibrillar meshwork lamina structure beneath the inner nuclear membrane (Fiserova *et al.*, 2009). KAKU4 (after the Japanese word for nucleus, *kaku*) is a candidate component of the plant nuclear lamina (Goto *et al.*, 2014; Meier *et al.*, 2017; Poulet *et al.*, 2017). In epidermal cells of the mature vegetative tissues of *A. thaliana*, a KAKU4-deificient mutant (*kaku4*) has smaller spherical-shaped nuclei, compared with spindle-shaped nuclei of the wild type. A spherical phenotype is also found in mutants defective in the outer nuclear membrane proteins WIPs (Zhou *et al.*, 2012), in the possible inner nuclear membrane proteins SUNs (Zhou *et al.*, 2012), and in the nuclear envelope-associated proteins CRWNs (CRWN1 and CRWN4) (Dittmer *et al.*, 2007; Goto *et al.*, 2014; Sakamoto and Takagi, 2013; Wang *et al.*, 2013).

In this study, we show that *KAKU4* is highly expressed in the VNs of pollen grains and tubes, resulting in deep invagination of the VN envelope. We propose that KAKU4-mediated deformation of the VN controls the proper migration order of VN and sperm cells during pollen tube growth in *A. thaliana*.

Materials and methods

Gene expression data from public databases

We assessed the gene expression level data in various tissues deposited in the database Atted-II (http://atted.jp/), and then downloaded the folder "Expression_data_Development" and used the file "AtGE_dev_gcRMA" which contains the raw data of microarray experiments (Schmid *et al.*, 2005). We chose the values of the genes of interest from wild-type plants for graphical presentation.

Plant materials

Arabidopsis thaliana (Columbia-0) was used as the wild-type line. T-DNA insertion mutants (SALK_076754 [*kaku4-2*], SALK_010298 [*kaku4-3*], SAIL_711_E09 [*kaku4-4*], and SALK_041774 [*crwn1-2*],) and EMS-mutagenized mutants (*kaku2* and *kaku4-1*) were isolated previously (Goto *et al.*, 2014). The transgenic plants *ProKAKU4:KAKU4-tRFP kaku4-2* and *ProKAKU4:KAKU4-EYFP kaku4-3*, in which the genomic fragment of the splice variant *KAKU4.2* was expressed, were also used (Goto *et al.*, 2014). Seeds were germinated and grown on MS medium containing 0.5% gellan gum at 22°C under continuous light (35 µmol m^{-2} s^{-1}). The plants were transferred to vermiculite in 2-3 weeks and grown at 22°C under a light cycle of 16 h light/8 h dark.

Plasmid construction and transformation using GUS under the KAKU4 promoter control

To construct *ProKAKU4:GUS*, a genomic fragment encompassing the 2-kb sequence upstream of the coding sequence was cloned into pENTR/D-TOPO (Invitrogen) and then fused upstream of *EGFP-GUS* in a plant transformation vector (pKGWFS7). The primers used for the amplification of the *KAKU4* promoter were the forward primer (5′-CACCGAGGAATACAGGCGAGAACA-3′) and the reverse primer (5′-GGTGAAAGTGAGAGGAGGAG-3′). The sequence motif 5′-CACC-3′ required for cloning into pENTR/D-TOPO was added at the 5′-end of the forward primer. To obtain stable expression, *Arabidopsis* wild-type plants were transformed with *Agrobacterium tumefaciens* (GV3101) using the floral dip method (Clough and Bent, 1998).

4

125

GUS staining

Floral organs were immersed in 90% acetone, and stored for one or two nights at -20°C. Then, 90% acetone was replaced by 1× phosphate buffer (100 mM $NaPO_4$; 10× stock solution [1M $NaPO_4$] was prepared by mixing 1M Na_2HPO_4 and 1M NaH_2PO_4 at a ratio of 61:39; 10× stock solution was diluted 10 times and used as 1× phosphate buffer), which was immediately replaced by the GUS-staining solution (100 mM $NaPO_4$ [pH 7.4], 10 mM EDTA, 0.1% Triton X-100, 1 mM potassium ferricyanide, 1 mM potassium ferrocyanide, 0.5 mg/mL 5-bromo-4-chloro-3-indolyl-β-D-glucuronide cyclohexylammonium). The GUS-staining solution was vacuum infiltrated into the floral organs for 5 min at 20-25°C. The floral organs infiltrated by the GUS-staining solution were incubated for 16 h in the dark at 37°C for GUS-staining reaction. The GUS-staining solution was replaced by 1× phosphate buffer, followed by rinsing with 70% ethanol two times. After rinsing, an ethanol and acetic acid mixture (ethanol : acetic acid = 6:1) was added for specimen preparation. The specimens were mounted with chloral hydrate solution (chloral hydrate: glycerol: water = 8 [g] : 1 [ml] : 2 [ml]) and examined using a differencial interference contrast microscope (DIC) (Axioskop 2 plus system [Carl Zeiss] and a high-sensitivity cooled CCD color camera VB-7010 [Keyence]).

Microscopy

Confocal fluorescence images except for those in Fig. 6 were obtained using a confocal laser scanning microscope (LSM780; Carl Zeiss). The 405 nm line of a blue diode laser, the 488 nm line of a 40 mW Ar/Kr laser, and the 544 nm line of a 1 mW He/Ne laser were used to excite Hoechst 33342, GFP/YFP, and RFP, respectively. Images were acquired with a ×63 1.2 NA water immersion objective (C-Apochromat, 441777-9970-000; Carl Zeiss), a ×40 0.95 NA dry objective (Plan-Apochromat, 440654-9902-000; Carl Zeiss), or a ×20 0.80 NA dry objective (Plan-Apochromat, 440640-9903-000; Carl Zeiss). Data were exported as TIFF files and processed using Adobe Photoshop Elements 9.0 (Adobe Systems) or ImageJ 1.45s (National Institutes of Health; NIH). Fluorescence images presented in Fig. 5A were obtained using an Axioskop2 plus microscope (Carl Zeiss) and a high-sensitivity cooled CCD color

5

157   camera VB-7010 (Keyence).

158

159   *Hoechst 33342 staining*

160   Pollen grains and pollen tubes were stained with a solution containing 1 µg/ml

161   Hoechst 33342, 3.7% (w/v) paraformaldehyde, 10% (v/v) dimethyl sulfoxide, 3% (v/v)

162   Nonidet P-40, 50 mM PIPES-KOH (pH 7.0), 1 mM $MgSO_4$, and 5 mM EGTA.

163

164   In vitro *pollen germination*

165   *In vitro* pollen germinations were performed as described previously (Boavida and

166   McCormick, 2007). Briefly, pollen grains from full-open flowers were transferred to the

167   medium on a glass slide by gently scraping the surface of the medium by a flower or

168   anthers. Three or four glass slides with the medium containing transferred pollen were

169   placed on Kim Wipes (produced by Nippon Paper Crecia based on partnership with

170   Kimberly Clark) in a square-shaped plastic petri dish (EIKEN CHEMICAL). Kim Wipes

171   wetted with water were put along the vertical wall of the dish to enclose the glass

172   slides before covering the dish with the lid. The petri dish was placed in an incubator

173   with temperature control set to 22°C and continuous light for 3–3.5 h, followed by

174   microscopic observation.

175

176   *Generation of double nuclear marker line for* in vitro *pollen tube growth assay*

177   pDM441, a binary vector harboring *ProLAT52:NLS-Clover* was generated as follows.

178   DNA fragment encoding mClover with A206K was amplified from a template plasmid

179   pPZP221 CloN (Takeuchi and Higashiyama, 2016) by a PCR using a primer set

180   pENTR_NLS_GFP (5'- CAC CAT GGC TCC AAA GAA GAA GAG AAA GGT CAT

181   GGT GAG CAA GGG CGA GGA G -3') and GFP_R (5'- CTT GTA CAG CTC GTC CAT

182   GCC G -3'). The PCR product was cloned into the pENTR/D-TOPO (Thermofisher) to

183   generate pOR003. LR recombination was performed between the pOR003 with a

184   modified pGWB501 (Nakagawa *et al.*, 2007) harboring *LAT52* promoter at the *Hind*III

185   site (Twell *et al.*, 1990) to produce the pDM441. Agrobacterium GV3101 containing

186   the pDM441 or *ProRPS5A:HISTONE 2B-tdTomato* (Maruyama *et al.*, 2013) were

187   independently cultured and subsequently used in simultaneous transformation by the

6

188 floral dip method (Clough and Bent, 1998) to generate double nuclear marker line

189 (*ProRPS5A:H2B-tdTomato ProLAT52:NLS-Clover*).

190

191 *Analysis of nuclear size and shape in pollen tubes in the microfluidic device*

192 Pollen grains from the *ProRPS5A:H2B-tdTomato ProLAT52:NLS-Clover* double

193 nuclear marker line were suspended in an *in vitro* pollen tube growth medium (Muro *et*

194 *al.*, 2018) without agarose and placed in a polydimethylsiloxane (PDMS) microfluidic

195 device on a glass slip (Matsunami). The PDMS microfluidic device with 10 μm-width of

196 micro channels was prepared as described previously (Yanagisawa *et al.*, 2017).

197 The device allows a pollen tube to elongate on a focal plane, resulting in easy imaging

198 analysis for hours. After 1h incubation at 22 ºC, fluorescence images of the nuclei

199 labeled with H2B-tdTomato and NLS-Clover in pollen tubes were obtained using a

200 confocal laser scanning microscope SP8 (Leica Microsystems). The images were

201 exported as TIFF files and processed using the Analyze Particles function of ImageJ.

202 A two-tailed homoscedastic Student's t test was performed using Microsoft Excel. The

203 circularity index was calculated using the equation $4\pi A/P^2$ (where A = area of nucleus

204 and P = perimeter of nucleus) and indicates how closely each nucleus corresponds to

205 a spherical shape (a perfect sphere has a circularity index of 1). Any deviation from a

206 circular shape (e.g., elongated, lobulated, or spindle shaped) causes the index to

207 decrease.

208

209 *Clearing siliques*

210 Fixation and clearing of siliques were performed as described previously (Chen *et al.*,

211 2015). Silique length was measured using ImageJ software.

212

213 *Reciprocal crosses*

214 F1 seeds from crosses between wild-type plants and *kaku4-3* hetero mutants

215 (*kaku4-3*/+) were sown on MS medium containing kanamycin sulfate at 70 μg/ml.

216 After 1-2 weeks, the live plants (Kan^R) and dead plants (Kan^S) were counted and

217 subjected to chi-squared tests.

218

7

219 *Accession numbers*

220 Sequence data from this article can be found in the Arabidopsis Genome Initiative or

221 EMBL/GenBank databases under the following accession numbers: *CRWN1*

222 (At1g67230), *CRWN2* (At1g13220), *CRWN3* (At1g68790), *CRWN4* (At5g65770),

223 *KAKU4* (At4g31430), *Myosin XI-i* (At4g33200), *Nup136* (At3g10650), *SUN1*

224 (At5g04990), *SUN2* (At3g10730), *WIP1* (At4g26455), *WIP2* (At5g56210), *WIP3*

225 (At3g13360), *WIT1* (At5g11390), and *WIT2* (At1g68910).

226

227

228 **Results**

229 *Remarkably high expression of* KAKU4 *in mature pollen grains*

230 By analyzing the gene-expression database of *A. thaliana* (ATTED-II, http://atted.jp/),

231 we found that *KAKU4*, which encodes a putative nuclear lamina protein, is highly

232 expressed in mature pollen (Fig. 1A) and that the high expression is specific to pollen

233 (Supplemental Fig. S1). Similarly, *WIT1*, which encodes an outer nuclear membrane

234 protein, is highly expressed in mature pollen (Fig. 1A) but it is also highly expressed in

235 seeds (Supplementary Fig. S1). Expressions of *WIT2* and *WIP3*, which encode other

236 nuclear membrane proteins, do not differ greatly among the tissues (Fig. 1A and

237 Supplementary Fig. S1).

238 To visualize the activity of the *KAKU4* promoter in mature pollen, we generated

239 transgenic plants expressing the β-glucuronidase (GUS) reporter gene under the

240 control of the *KAKU4* promoter. Strong GUS signals were detected in pollen grains of

241 the anthers (Fig. 1B, upper panels) and pollen tubes elongating into the stigma (Fig.

242 1B, lower panels). These results indicate that *KAKU4* is predominantly expressed in

243 mature pollen grains.

244

245 *KAKU4 is highly abundant on the VN envelope and less abundant on the SCN*

246 *envelope in pollen grains*

247 We examined the subcellular localization of the KAKU4 protein in mature pollen grains

248 with the fluorescent KAKU4 markers. To avoid overexpression of the transgenes,

249 KAKU4-tRFP and KAKU4-EYFP were expressed in the *KAKU4*-deficient mutant

250 alleles *kaku4-2* and *kaku4-3*, respectively, under the control of the native promoter.

251 Fluorescence signals of KAKU4-tRFP were clearly detected at the VN of each pollen

252 grain (Fig. 2A). At a higher magnification, the fluorescence images showed that

253 KAKU4-tRFP was localized to the nuclear envelope of the VN that were stained with

254 Hoechst 33342 (Fig. 2B, upper panels). With an increased imaging sensitivity,

255 KAKU4-tRFP was also detected on the envelope of two SCNs that were stained with

256 Hoechst 33342 (Fig. 2B, lower panels, arrows). Similar results were obtained with

257 KAKU4-EYFP (see Fig. 3A). The fluorescence levels of the SCNs were much lower

258 than those of the VNs (Fig. 2B and Fig. 3A). Hence, KAKU4 is more densely

259 accumulated in the envelopes of the VNs than in the envelopes of the SCNs.

260

261 *The dense accumulation of KAKU4 leads to deformation of the VN*

262 The nuclear shapes were compared between the SCN and the VN in the transgenic

263 plants that expressed KAKU4-EYFP in *kaku4-3* under the control of the native

264 promoter. The SCNs were nearly spherical in shape and their envelopes were

265 relatively smooth (Fig. 3A). On the other hand, the VN were deeply invaginated (Fig.

266 3A). The deformation features of the VN are very similar to those of the nuclei in

267 seedlings overexpressing KAKU4-GFP, in which artificial overexpression of KAKU4

268 causes nuclear envelope deformation in a dose-dependent manner (Goto *et al.*, 2014).

269 This implied that the VN deformation is due to hyperaccumulation of KAKU4 on their

270 envelopes.

271 Next, the effect of *KAKU4* deficiency on the deformation degrees of the VNs was

272 examined with pollen grains from the wild type and the *kaku4* mutant alleles. The

273 shapes of the VNs stained with Hoechst 33342 were classified into two types:

274 spherical and non-spherical (Fig. 3B). Non-spherical shapes included elongated

275 shapes and distorted shapes. The proportions of non-spherical shaped VNs were

276 significantly lower in both *kaku4-3* and *kaku4-4* than in the wild type (Fig. 3C). Taken

277 together, this result indicates that KAKU4 has a role in modulating nuclear shape in

278 pollen.

279

280 *Involvement of KAKU4 in controlling the migration order of VN and SCNs in*

281 *elongating pollen tubes*

9

282 After pollination, a pollen grain germinates and elongates to form a pollen tube, in

283 which the VN and the SCNs migrate towards the ovules (Kawashima and Berger,

284 2011). Using transgenic plants that expressed KAKU4-tRFP in *kaku4-2* under the

285 native promoter and an *in-vitro* pollen germination assay (Boavida and McCormick,

286 2007), we were able to observe the KAKU4-labeled VN and the two SCNs migrating

287 towards the tip of elongating pollen tubes (Fig. 4A, left). Like the nuclei in pollen grains,

288 the VN envelopes highly fluoresced, while the SCN envelopes moderately fluoresced

289 (Fig. 4A, right). Similar observations were made with another transgenic plant that

290 expressed KAKU4-EYFP in *kaku4-3* under the native promoter (Fig. 4B). In most

291 elongating pollen tubes, the VN preceded the two SCNs (Fig. 4).

292 To quantitatively analyze the migration order of the VNs and the SCNs,

293 elongating pollen tubes were categorized into three types: (1) the VN-first type, in

294 which the VN preceded the two SCNs (Fig. 5A, upper), (2) the SCN-first type, in which

295 the two SCNs preceded the VN (Fig. 5A, lower), and (3) the together type, in which

296 VN and SCN were close to each other. Most of the wild type pollen tubes (91–93 %)

297 were VN-first type (Fig. 5B). The proportions of VN-first type were markedly reduced

298 to 33–52% in three *kaku4* mutant alleles (Fig. 5B), indicating that the control of the

299 migration order of the VN and the SCNs in pollen tubes was impaired in the *kaku4*

300 mutant alleles.

301 We next examined an effect of deficiency of the KAKU4-interacting protein

302 CRWN1 (Dittmer *et al.*, 2007; Sakamoto and Takagi, 2013) on the migration order by

303 using two mutant alleles (*crwn1-2 and kaku2*) (Goto *et al.*, 2014). The proportions of

304 the VN-first type in these mutant alleles (77-87%) were slightly lower than those of the

305 wild type (Fig. 5B). Taken together, these results suggest that the nuclear lamina

306 candidate proteins KAKU4 and CRWN1 control the migration order of the VN and

307 SCNs in elongating pollen tubes, in which KAKU4 functions more predominantly than

308 CRWN1.

309 We next compared the nuclear shape and size in the elongating pollen tubes

310 between the wild-type and *kaku4-3* plants, by visualizing the VNs and the SCNs with a

311 nuclear marker (H2B-tdTomato) under the constitutive promoter and by visualizing the

312 VNs with another nuclear marker (NLS-Clover) under the VN-specific promoter. The

313 SCNs exhibited moderate difference in the sizes and shapes between the wild type

314 and *kaku4-3* (Fig. 6A and Supplemental Fig. S2). On the contrary, compared with the

10

315   *kaku4-3* VNs, the wild-type VNs were larger and highly invaginated (Fig. 6A). To

316   quantitatively evaluate the degree of nuclear deformation, we calculated a circularity

317   index ($4\pi A/P^2$; where A = area of nucleus and P = perimeter of nucleus). The VN

318   circularity index was much smaller for the wild-type than it was for *kaku4-3* in both VN-

319   and SCN-first-type pollen tubes (Fig. 6B, upper). This result indicates that the

320   wild-type VNs are more deformed than the *kaku4-3* VNs. In addition, the fluorescence

321   area of the VNs was larger in the wild-type VNs than in *kaku4-3* (Fig. 6B, lower).

322   Notably, the *kaku4-3* VNs of VN-first-type pollen tubes were significantly smaller than

323   those of the SCN-first-type tubes, although the circularity indices of the VNs of both

324   types of pollen tubes were not significantly different (Fig. 6B). This indicates that

325   having a small size makes it easier for the VNs to precede the sperm cells in

326   elongating pollen tubes.

327

328   *Slightly decreased seed production and lower pollen competitive ability in* kaku4

329   The preceding observations raised the question of whether the migration order of VN

330   and SCN has an effect on fertilization. To assess the effect of *KAKU4* deficiency on

331   fertilization, we analyzed the seed numbers and the silique lengths in the wild type

332   and *kaku4* mutant alleles (Fig. 7A). The number of seeds per silique of the *kaku4*

333   mutant alleles *kaku4-2* and *kaku4-3* was moderately decreased to 82% and 87%,

334   respectively, as compared to that number of the wild type (Fig. 7B). The silique was 1

335   mm shorter in the *kaku4* mutants, than in wild-type plants (Fig. 7C). These results

336   indicate that *KAKU4* contributed to efficient seed production and proper fruit

337   development.

338   To test whether the seed reduction in *kaku4* was paternally controlled, we

339   reciprocally crossed between wild-type plants and the heterozygous *kaku4-3*/+ mutant.

340   The *KAKU4* mutant gene in *kaku4-3* carries a kanamycin resistance gene insert. As

341   shown in Table 1, when *kaku4-3*/+ was used as pollen donor to the wild type, the

342   number of kanamycin-resistant progeny was significantly smaller than expected,

343   indicating a reduced pollen competitive ability of *kaku4*. When the wild type was used

344   as the pollen donor to *kaku4-3*/+, the number of kanamycin-resistant progeny did not

345   significantly differ from the expected values. This suggests that *KAKU4* has little or no

346   involvement in functions of pistils in reproduction. Taken together, these results

347   suggest that the VN precedence over SCs in pollen tubes contributes to maintaining

11

348   proper male transmission efficiency in seed production.

349

350

351   **Discussion**

352   In wild-type pollen tubes, the migration order of VN and sperm cells is mostly

353   maintained during their migration, although it occasionally changes (Zhou and Meier,

354   2014). This implies that the initial positions of the VN and sperm cells when they move

355   from the pollen grain to the pollen tube is important for the VN precedent migration

356   over the two-sperm-cell unit that is surrounded by a membrane (Li *et al.*, 2013;

357   Sprunck *et al.*, 2014; Wudick *et al.*, 2018). In wild-type pollen tubes, the VN enters the

358   pollen tube earlier than sperm cells even though it is expected to be larger than the

359   two sperm cells combined (Mcconchie *et al.*, 1987). In this study, *KAKU4* deficiency

360   causes the losses of 1) the irregularity in VN shape and 2) the control of migration

361   order of VN and sperm cells at the same time, suggesting that the VN deformation

362   ability is related to the migration order in the pollen tube. Our observations of wild-type

363   pollen grains showed that VN envelope was deeply invaginated inside the nucleus

364   and that VN shapes were elongated in the pollen tube. These features might allow the

365   VN to easily enter the pollen tube. Hence, we propose that a KAKU4-dependent ability

366   to elongate the VN shapes increases the probability that VN will enter the pollen tube

367   first, resulting in the VN precedent migration over sperm cells in pollen tubes.

368   Two studies have shown that depolymerization of microtubules can affect the

369   migration order of the VN and sperm cells (Astrom *et al.*, 1995; Heslopharrison *et al.*,

370   1988). In *Galanthus nivalis* pollen tubes, microtubule depolymerization with colchicine

371   caused a large increase in the "generative cell lead" (referred to as "SCN first" in this

372   study) (Heslopharrison *et al.*, 1988), and in *Nicotiana tabacum* pollen tubes,

373   microtubule depolymerization with oryzalin caused a decrease in pollen tubes

374   harboring VN and an increase in pollen tubes harboring generative cells (sperm cells)

375   (Fig. 5 in Astrom et al., 1995). The loss of two proteins essential for the recruitment of

376   γ-tubulin complexes at microtubule organizing centers (GIP1 and GIP2) alters nuclear

377   shape in root tips (Batzenschlager *et al.*, 2013). These results, together with our data,

378   raises the possibility that microtubule depolymerization may cause a change in

379   nuclear shape, which affects the migration order of VN and sperm cells.

380   While the VN preceded the sperm cells in the majority of wild-type pollen tubes,

381 the sperm cells preceded the VN in the majority of the pollen tubes in multiple mutant

382 alleles of *wip*, *wit*, *wifi* (Zhou and Meier, 2014), and the *sun* mutant line expressing a

383 dominant-negative gene, in which WIP1 and WIT1 were delocalized from the VN

384 envelope (*Lat52pro::ERS-RFP-SUN2Lm sun1-KO sun2-KD*) (Zhou *et al.*, 2015).

385 These studies indicate that WIPs and WITs are needed to control the migration order

386 of VN and sperm cells in pollen tubes. VNs were reported to be normal in multiple

387 mutants deficient in *WIPs* and/or *WITs* (*wip*, *wit*, and *wifi*) (Zhou and Meier, 2014).

388 However, we cannot exclude the possibility that shape of VN in the mutants' pollen

389 differs from that in wild-type pollen. The nuclear shape in the leaves and root hairs of

390 the *wip* mutant allele is similar to that in *kaku4* (Zhou *et al.*, 2012). However, because

391 the ratio of "VN first" and "SCN first" is very different between the *wip/wit/wifi* and

392 *kaku4* mutants, the underlying mechanism affecting the migration order of VN and

393 SCNs may be different between WIP/WIT and KAKU4.

394   Defects in the migration order of VN and sperm cells in *wip/wit/wifi* (Zhou and

395 Meier, 2014) and *kaku4* (this study) caused a decrease in seed reproduction, which

396 suggests that positioning VN first in the pollen tubes is important. In mutants deficient

397 in *WIPs* and/or *WITs*, the pollen tubes frequently failed to properly elongate, to burst at

398 the tube tips, and to result in fertilization (Zhou and Meier, 2014). These observations

399 suggest that the proximity of the VN to the growing pollen tube tip is probably critical

400 for pollen tube reception (Zhou and Meier, 2014). The number of seeds in *kaku4*

401 mutants was ~80% of that in wild-type plants (Fig. 7B). This result suggests that

402 *KAKU4* deficiency does not cause severe defects in pollen tube growth and

403 fertilization. One possible explanation for the impaired competitive ability of pollen in

404 *kaku4* is that the elongation speed of SCN-first-type pollen tubes might be slightly

405 lower than that of VN-first-type pollen tubes. Positioning of VN close to the tip may

406 contribute to efficient elongation of pollen tubes.

407

408

409 **Supplementary data**

410 The following materials are available in the online version of this article.

411 **Supplementary Fig. S1.** Expression of *KAKU4, WIT1, WIT2, and WIP3*.

412 **Supplementary Fig. S2.** Nuclear shape and size of SCN in pollen tubes of *kaku4.*

13

413

Acknowledgements

424

References

Astrom H, Sorri O, Raudaskoski M. 1995. Role of Microtubules in the Movement of the Vegetative Nucleus and Generative Cell in Tobacco Pollen Tubes. Sexual Plant Reproduction **8**, 61-69.

Batzenschlager M, Masoud K, Janski N, Houlne G, Herzog E, Evrard JL, Baumberger N, Erhardt M, Nomine Y, Kieffer B, Schmit AC, Chaboute ME. 2013. The GIP gamma-tubulin complex-associated proteins are involved in nuclear architecture in Arabidopsis thaliana. Front Plant Sci **4**, 480.

Boavida LC, McCormick S. 2007. Temperature as a determinant factor for increased and reproducible in vitro pollen germination in Arabidopsis thaliana. Plant Journal **52**, 570-582.

Borg M, Twell D. 2011. Pollen: Structure and Development. In: eLS. John Wiley & Sons, Ltd: Chichester.

Chen LQ, Lin IW, Qu XQ, Sosso D, McFarlane HE, Londono A, Samuels AL, Frommer WB. 2015. A cascade of sequentially expressed sucrose transporters in the seed coat and endosperm provides nutrition for the Arabidopsis embryo. Plant Cell **27**, 607-619.

Clough SJ, Bent AF. 1998. Floral dip: a simplified method for *Agrobacterium*-mediated transformation of *Arabidopsis thaliana*. Plant J **16**, 735-743.

Dittmer TA, Stacey NJ, Sugimoto-Shirasu K, Richards EJ. 2007. LITTLE NUCLEI genes affecting nuclear morphology in Arabidopsis thaliana. Plant Cell **19**, 2793-2803.

Fiserova J, Kiseleva E, Goldberg MW. 2009. Nuclear envelope and nuclear pore complex structure and organization in tobacco BY-2 cells. Plant J **59**, 243-255.

Goto C, Tamura K, Fukao Y, Shimada T, Hara-Nishimura I. 2014. The Novel Nuclear Envelope Protein KAKU4 Modulates Nuclear Morphology in Arabidopsis. Plant Cell **26**, 2143-2155.

Hamamura Y, Saito C, Awai C, Kurihara D, Miyawaki A, Nakagawa T, Kanaoka MM, Sasaki N, Nakano A, Berger F, Higashiyama T. 2011. Live-cell imaging reveals the dynamics of two sperm cells during double fertilization in Arabidopsis thaliana. Curr Biol **21**, 497-502.

Heslopharrison J, Heslopharrison Y, Cresti M, Tiezzi A, Moscatelli A. 1988. Cytoskeletal Elements, Cell Shaping and Movement in the Angiosperm Pollen-Tube. Journal of Cell Science **91**, 49-60.

Kawashima T, Berger F. 2011. Green love talks; cell-cell communication during double fertilization in flowering plants. AoB Plants **2011**, plr015.

Li S, Zhou LZ, Feng QN, McCormick S, Zhang Y. 2013. The C-terminal hypervariable domain targets Arabidopsis ROP9 to the invaginated pollen tube plasma membrane. Mol Plant **6**, 1362-1364.

Maruyama D, Hamamura Y, Takeuchi H, Susaki D, Nishimaki M, Kurihara D, Kasahara RD, Higashiyama T. 2013. Independent Control by Each Female Gamete Prevents the Attraction of Multiple Pollen Tubes. Developmental Cell **25**, 317-323.

Maruyama D, Volz R, Takeuchi H, Mori T, Igawa T, Kurihara D, Kawashima T, Ueda M, Ito M, Umeda M, Nishikawa S, Gross-Hardt R, Higashiyama T. 2015. Rapid Elimination of the Persistent Synergid through a Cell Fusion Mechanism. Cell **161**, 907-918.

Mcconchie CA, Russell SD, Dumas C, Tuohy M, Knox RB. 1987. Quantitative Cytology of the Sperm Cells of Brassica-Campestris and Brassica-Oleracea. Planta **170**, 446-452.

McCue AD, Cresti M, Feijo JA, Slotkin RK. 2011. Cytoplasmic connection of sperm cells to the pollen vegetative cell nucleus: potential roles of the male germ unit revisited. Journal of Experimental Botany **62**, 1621-1631.

Meier I, Richards EJ, Evans DE. 2017. Cell Biology of the Plant Nucleus. Annu Rev Plant Biol **68**, 139-172.

Muro K, Matsuura-Tokita K, Tsukamoto R, Kanaoka MM, Ebine K, Higashiyama T, Nakano A, Ueda T. 2018. ANTH domain-containing proteins are required for the pollen tube plasma membrane integrity via recycling ANXUR kinases. Communications Biology **1**.

Nakagawa T, Suzuki T, Murata S, Nakamura S, Hino T, Maeo K, Tabata R, Kawai T, Tanaka K, Niwa Y, Watanabe Y, Nakamura K, Kimura T, Ishiguro S. 2007. Improved gateway binary vectors: High-performance vectors for creation of fusion constructs in Transgenic analysis of plants. Bioscience Biotechnology and Biochemistry **71**, 2095-2100.

Poulet A, Probst AV, Graumann K, Tatout C, Evans D. 2017. Exploring the evolution of the proteins of the plant nuclear envelope. Nucleus **8**, 46-59.

Sakamoto Y, Takagi S. 2013. LITTLE NUCLEI 1 and 4 regulate nuclear morphology in Arabidopsis thaliana. Plant Cell Physiol **54**, 622-633.

Schmid M, Davison TS, Henz SR, Pape UJ, Demar M, Vingron M, Scholkopf B, Weigel D, Lohmann JU. 2005. A gene expression map of Arabidopsis thaliana

development. Nat Genet **37**, 501-506.

Sprunck S, Hackenberg T, Englhart M, Vogler F. 2014. Same same but different: sperm-activating EC1 and ECA1 gametogenesis-related family proteins. Biochem Soc Trans **42**, 401-407.

Takeuchi H, Higashiyama T. 2016. Tip-localized receptors control pollen tube growth and LURE sensing in Arabidopsis. Nature **531**, 245-248.

Tamura K, Iwabuchi K, Fukao Y, Kondo M, Okamoto K, Ueda H, Nishimura M, Hara-Nishimura I. 2013. Myosin XI-i links the nuclear membrane to the cytoskeleton to control nuclear movement and shape in Arabidopsis. Curr Biol **23**, 1776-1781.

Twell D, Yamaguchi J, Mccormick S. 1990. Pollen-Specific Gene-Expression in Transgenic Plants - Coordinate Regulation of 2 Different Tomato Gene Promoters during Microsporogenesis. Development **109**, 705-713.

Vogler F, Konrad SSA, Sprunck S. 2015. Knockin' on pollen's door: live cell imaging of early polarization events in germinating Arabidopsis pollen. Frontiers in Plant Science **6**.

Wang H, Dittmer TA, Richards EJ. 2013. Arabidopsis CROWDED NUCLEI (CRWN) proteins are required for nuclear size control and heterochromatin organization. BMC Plant Biol **13**, 200.

Wudick MM, Portes MT, Michard E, Rosas-Santiago P, Lizzio MA, Nunes CO, Campos C, Santa Cruz Damineli D, Carvalho JC, Lima PT, Pantoja O, Feijo JA. 2018. CORNICHON sorting and regulation of GLR channels underlie pollen tube Ca(2+) homeostasis. Science **360**, 533-536.

Yanagisawa N, Sugimoto N, Arata H, Higashiyama T, Sato Y. 2017. Capability of tip-growing plant cells to penetrate into extremely narrow gaps. Sci Rep **7**, 1403.

Zhou X, Graumann K, Evans DE, Meier I. 2012. Novel plant SUN-KASH bridges are involved in RanGAP anchoring and nuclear shape determination. J Cell Biol **196**, 203-211.

Zhou X, Groves NR, Meier I. 2015. SUN anchors pollen WIP-WIT complexes at the vegetative nuclear envelope and is necessary for pollen tube targeting and fertility. Journal of Experimental Botany **66**, 7299-7307.

Zhou X, Meier I. 2014. Efficient plant male fertility depends on vegetative nuclear movement mediated by two families of plant outer nuclear membrane proteins. Proceedings of the National Academy of Sciences of the United States of America **111**, 11900-11905.

Table1. Genetic assay of male transmission in *kaku4-3*/+ mutant by reciprocal crosses.

Female parent	Male parent	Kan^R	Kan^S	Kan^R/Kan^S	χ^2	TE$_f$	TE$_m$
kaku4-3/+	*kaku4-3*/+	280	84	3.33333	0.39682	NA	NA
wild type	*kaku4-3*/+	83	145	0.57241	0.00004	NA	57%
kaku4-3/+	wild type	126	129	0.97674	0.85098	98%	NA

Kan^R, kanamycin-resistant; Kan^S, kanamycin-sensitive; TE, transmission efficiency; TE = Kan^R/Kan^S (%); TE$_f$, female transmission; TE$_m$, male transmission; NA, not applicable.

Figure legends

Fig. 1. Expression of *KAKU4* in pollen.

(A) Transcript levels of *KAKU4*, *WIT1*, *WIT2* and *WIP3* in various tissues. Data were obtained from the website of the AtGenExpress project (http://jsp.weigelworld.org/AtGenExpress/resources/) (Schmid et al. 2005). Intensities (absolute values) from some tissues (see the website for details) were extracted and the means ± SE are shown. The data for *WIP1* and *WIP2* were not available. See also Supplementary Fig.1 for the values from more tissues.

(B) β-Glucuronidase (GUS) reporter assay of heterozygous transgenic plants that expressed GUS gene under the control of *KAKU4* promoter.

(B-1) GUS-stained flowers. (B-2) Enlarged image of the anther. (B-3) Pollen attached to a stigma. (B-4) Enlarged image of the stigma in B-3. Some of the pollen grains are not stained because the tested line carries the heterozygous transgene (B-4). Scale bars = 500 μm in B-1 and 100 μm in B-2 to B-4.

Fig. 2. Subcellular localization of KAKU4 to the nuclear envelope in pollen grains.

(A) Pollen grains from *kaku4-2* expressing *KAKU4-tRFP* under the control of *KAKU4* promoter. Magenta, tRFP; Green, autofluorescence.

(B) Two sets of enlarged images of pollen grains from *kaku4-2* expressing *KAKU4-tRFP* (upper and lower). The pollen grains were stained with Hoechst 33342. Arrows indicate SCNs.

Fig. 3. Nuclear shape of VN in pollen grains of *kaku4*

(A) A pollen grain from *kaku4-3* expressing *KAKU4-EYFP* under the control of *KAKU4* promoter. Two sets of images with high and low digital gain (upper and lower panels, respectively) are shown. Arrows indicate SCNs. Note that the VN has invaginated nuclear envelope inside, while the SCNs have not.

(B) Fluorescence images of nuclei stained with Hoechst 33342 in pollen grains. Non-spherical type, a pollen grain whose VN is irregularly shaped. Spherical type, a pollen grain of which VN is spherically shaped.

(C) Proportions of VN with non-spherical shape and VN with spherical shape each for wild-type pollen and *kaku4* pollen. In total, 51 (wild type), 100 (*kaku4-3*), and 61

(kaku4-4) pollen grains were tested.

Fig. 4. Nuclear envelope localization of KAKU4 in elongating pollen tubes.

(A) A pollen tube from *kaku4-2* expressing *KAKU4-tRFP* under the control of *KAKU4* promoter. This image was taken after 3 h of incubation using the *in-vitro* pollen germination system. The areas surrounded by dashed lines are enlarged on the right side.

(B) A pollen tube from *kaku4-3* expressing *KAKU4-EYFP* under the control of *KAKU4* promoter. This image was taken after 3.5 h of incubation using the *in-vitro* pollen germination system. The pollen tube elongates toward the right of the panels. Arrows indicate SCNs. DIC, differential interference contrast.

Fig. 5. Position of VN and SCN in pollen tubes of *kaku4.*

(A) (Left) Representative fluorescence images of nuclei in pollen tubes stained with Hoechst 33342. (Right) Diagrams of the photos showing the VN and two SCNs in pollen tubes. The diagrams are after Sprunck et al. 2014.

(B) Relative positions of VN and SCNs in wild-type, *kaku4* or *kaku2/crwn1* pollen tubes. Pollen grains were germinated on artificial medium at 22 °C. The pollen tubes were fixed and stained with Hoechst 33342 after 3 h (for wild type, *kaku4-3*, *kaku4-4*, and *crwn1-2*) or 3.5 h (for wild type*, *kaku4-1* and *kaku2*) of incubation. The relative positions were categorized as VN-first type (VN is ahead of SCN), SCN-first type (SCNs are ahead of VN); and Together type (VN and SCN are close). In total, 55 (wild type), 50 (*kaku4-3*), 66 (*kaku4-4*), 31 (*crwn1-2*), 45 (wild type*), 18 (*kaku4-1*), and 26 (*kaku2 [crwn1]*) pollen tubes were tested. Wild type*, a transgenic plant expressing Nup50a-GFP (parental line of *kaku4-1* and *kaku2*).

Fig. 6. Nuclear shape and size of VN in pollen tubes of *kaku4.*

(A) Representative fluorescence images of pollen tubes from the double nuclear marker line, in which the VNs were labeled with H2B-tdTomato (magenta) and NLS-Clover (green) and the SCNs were labeled with H2B-tdTomato (magenta). The pollen tubes were elongated in 10-µm-wide and 4-µm-depth channels of a polydimethylsiloxane microfluidic device and were analyzed after 1 h of incubation at 22 ºC.

20

(B) Circularity indices and areas of the VN in the VN-first-type pollen tubes of the wild-type plants and in the VN- and SCN-first-type pollen tubes of *kaku4-3* plants. Wild-type pollen tubes showed only VN-first-type positioning. The circularity index is defined as the equation $4\pi A/P^2$ (where A = area of nucleus and P = perimeter of nucleus) and indicates how closely each nucleus corresponds to a spherical shape (a perfect sphere has a circularity index of 1). Any deviation from a circular shape (e.g., elongated, lobulated, or spindle shaped) causes the index to decrease. Means ± standard errors for n = 16 (wild type), 18 (*kaku4-3* VN-first), or 16 (*kaku4-3* SCN-first). Asterisks indicate a significant difference (Student's *t* test, **P < 0.001, *P < 0.005).

Fig. 7. Seed production in *kaku4*.

(A) Representative photographs of siliques of wild-type plant, *kaku4-2*, and *crwn1-2*. Bars = 1 mm.

(B) Number of seeds per silique from wild-type plant, *kaku4-2*, and *crwn1-2* (means ± standard errors for n = 60) (left) and the number of seeds per silique from wild-type plant and *kaku4-3* (means ± standard errors for n = 59 [wild-type] or 55 [*kaku4-3*]) (right).

(C) Length of the siliques from wild-type plant, *kaku4-2*, and *crwn1-2* (means ± standard errors for n = 23 [wild-type], 22 [*kaku4-2*], or 27 [*crwn1-2*]) (left) and length of the siliques from wild-type plant and *kaku4-3* (means ± standard errors for n = 62 [wild-type] or n = 55 [*kaku4-3*]) (right).

Asterisks indicate a significant difference from wild type (Student's *t* test, *P < 0.05).

Supplementary Fig. S1. Expression of *KAKU4, WIT1, WIT2, and WIP3*. Transcript levels of *KAKU4*, *WIT1*, *WIT2* and *WIP3* in various tissues. Data were obtained from the resource page of the AtGenExpress project (http://jsp.weigelworld.org/AtGenExpress/resources/) (Schmid et al. 2005). Intensities (absolute values) from select tissues of wild-type plants are shown.

Supplementary Fig. S2. Nuclear shape and size of SCN in pollen tubes of *kaku4.* Circularity indices and areas of SCNs in the VN-first-type pollen tubes of the wild-type plants and in the VN- and SCN-first-type pollen tubes of *kaku4-3* plants. Wild-type pollen tubes showed only VN-first-type positioning. The circularity index is defined as

the equation $4\pi A/P^2$ (where A = area of nucleus and P = perimeter of nucleus). Means ± standard errors for n = 16 (wild type), 18 (*kaku4-3* VN-first), or 16 (*kaku4-3* SCN-first). Asterisks indicate a significant difference (Student's t test, **$P < 0.001$, *$P < 0.005$).
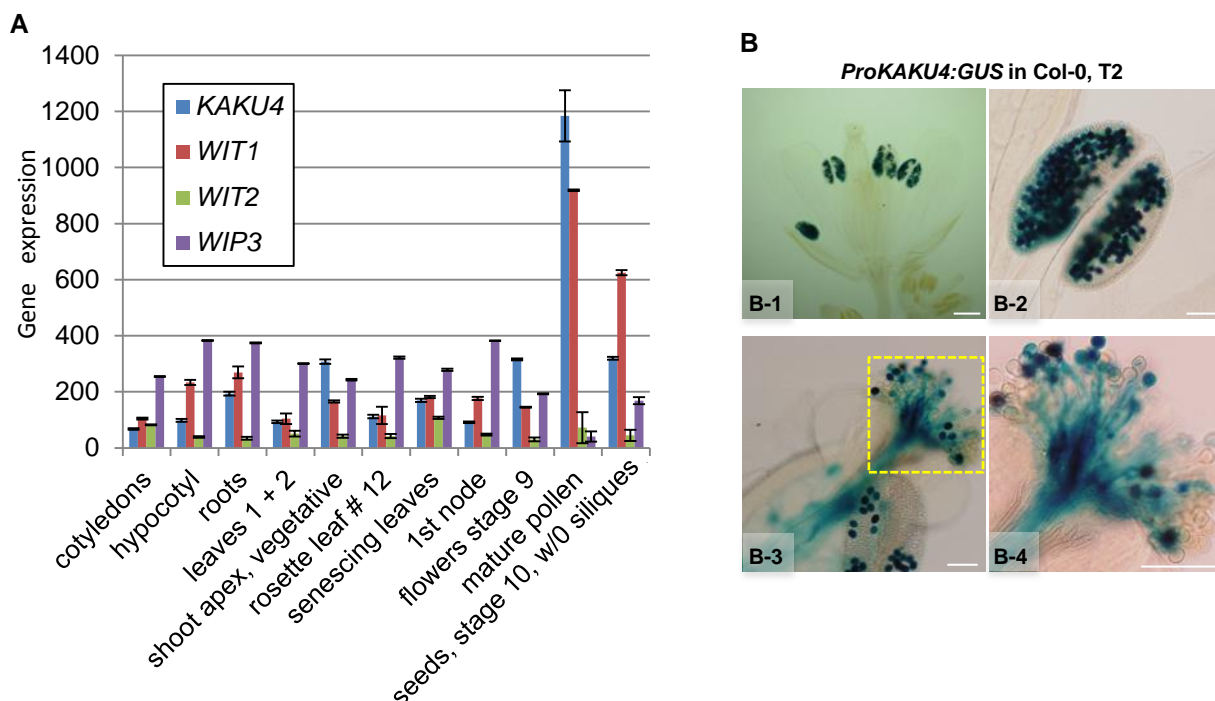
A

B

ProKAKU4:GUS in Col-0, T2

Fig. 1. Expression of *KAKU4* in pollen.

(A) Transcript levels of *KAKU4*, *WIT1*, *WIT2* and *WIP3* in various tissues. Data were obtained from the website of the AtGenExpress project (http://jsp.weigelworld.org/AtGenExpress/resources/) (Schmid et al. 2005). Intensities (absolute values) from some tissues (see the website for details) were extracted and the means ± SE are shown. The data for *WIP1* and *WIP2* were not available. See also Supplementary Fig.1 for the values from more tissues.

(B) β-Glucuronidase (GUS) reporter assay of heterozygous transgenic plants that expressed GUS gene under the control of *KAKU4* promoter.

(B-1) GUS-stained flowers. (B-2) Enlarged image of the anther. (B-3) Pollen attached to a stigma. (B-4) Enlarged image of the stigma in B-3. Some of the pollen grains are not stained because the tested line carries the heterozygous transgene (B-4) . Scale bars = 500 μm in B-1 and 100 μm in B-2 to B-4.
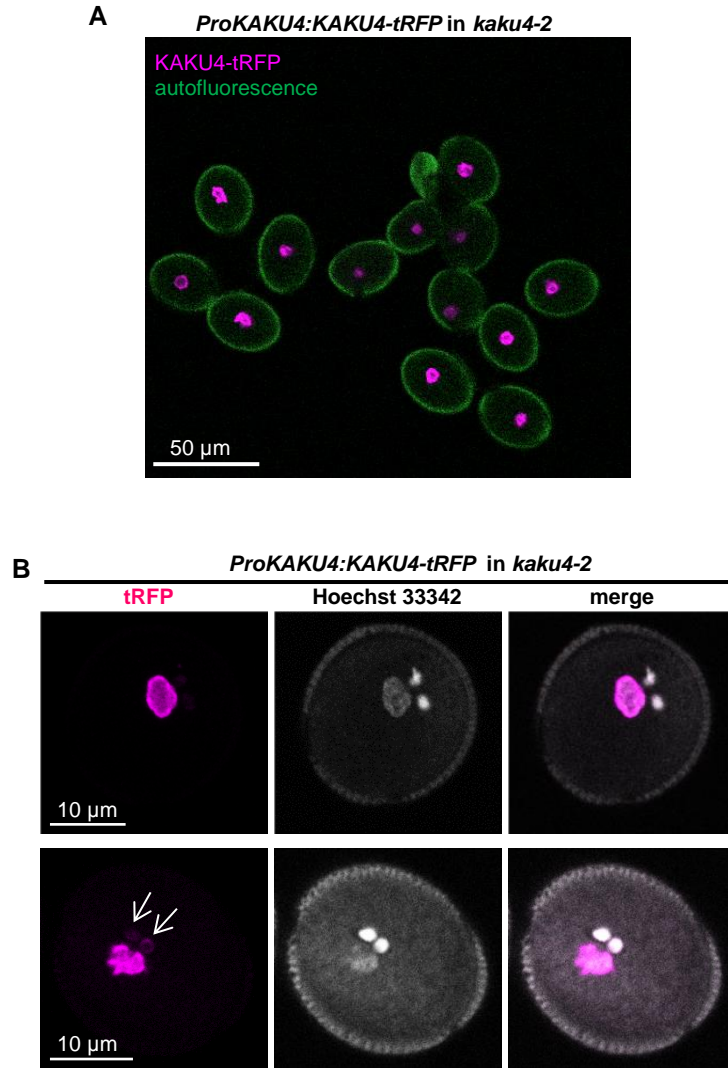
A *ProKAKU4:KAKU4-tRFP* in *kaku4-2*

KAKU4-tRFP
autofluorescence

50 µm

B *ProKAKU4:KAKU4-tRFP* in *kaku4-2*

| tRFP | Hoechst 33342 | merge |

10 µm

10 µm

Fig. 2. Subcellular localization of KAKU4 to the nuclear envelope in pollen grains.
(A) Pollen grains from *kaku4-2* expressing *KAKU4-tRFP* under the control of *KAKU4* promoter.
Magenta, tRFP; Green, autofluorescence.
(B) Two sets of enlarged images of pollen grains from *kaku4-2* expressing *KAKU4-tRFP* (upper and lower). The pollen grains were stained with Hoechst 33342. Arrows indicate SCNs.

A *ProKAKU4:KAKU4-EYFP* in *kaku4-3*

B Non-spherical type   Spherical type

C □ Non-spherical ■ Spherical

Fig. 3. Nuclear shape of VN in pollen grains of *kaku4*
(A) A pollen grain from *kaku4-3* expressing *KAKU4-EYFP* under the control of *KAKU4* promoter.
Two sets of images with high and low digital gain (upper and lower panels, respectively) are
shown. Arrows indicate SCNs. Note that the VN has invaginated nuclear envelope inside, while
the SCNs have not.
(B) Fluorescence images of nuclei stained with Hoechst 33342 in pollen grains. Non-spherical
type, a pollen grain whose VN is irregularly shaped. Spherical type, a pollen grain of which VN
is spherically shaped.
(C) Proportions of VN with non-spherical shape and VN with spherical shape each for wild-type
pollen and *kaku4* pollen. In total, 51 (wild type), 100 (*kaku4-3*), and 61 *(kaku4-4*) pollen grains
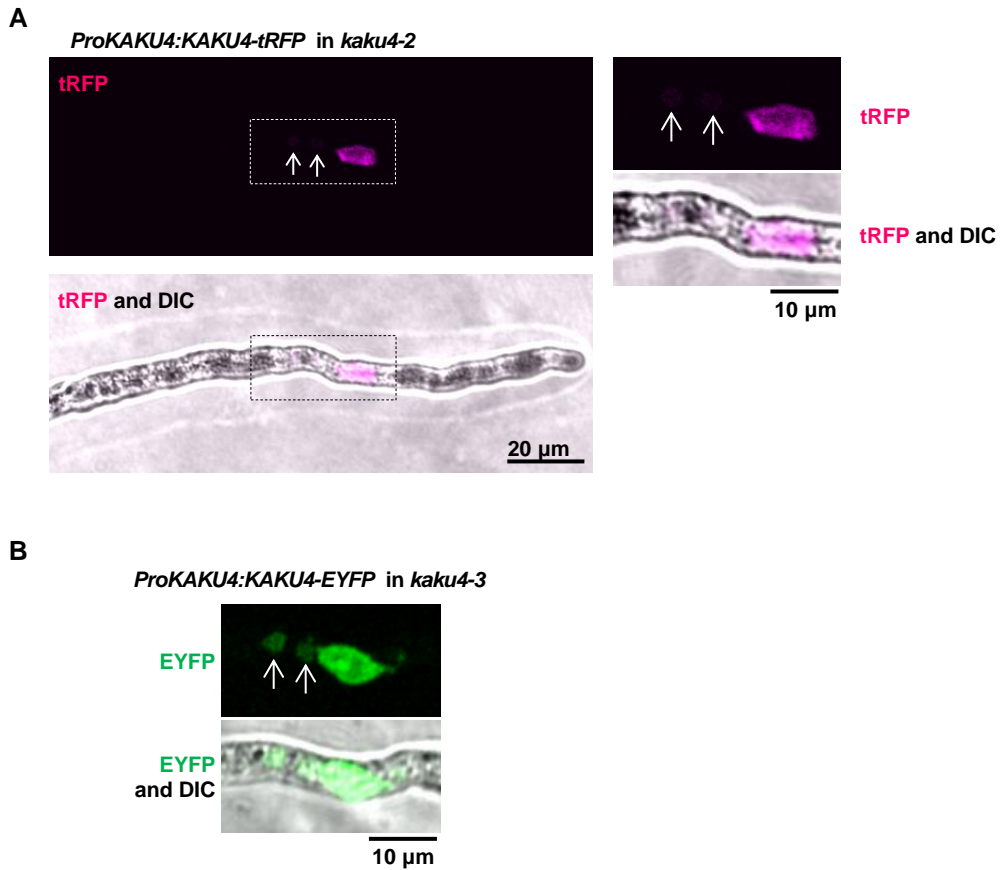were tested.

A

ProKAKU4:KAKU4-tRFP in *kaku4-2*

tRFP

tRFP and DIC

tRFP

tRFP and DIC

10 µm

20 µm

B

ProKAKU4:KAKU4-EYFP in *kaku4-3*

EYFP

EYFP and DIC

10 µm

Fig. 4. Nuclear envelope localization of KAKU4 in elongating pollen tubes.
(A) A pollen tube from *kaku4-2* expressing *KAKU4-tRFP* under the control of *KAKU4* promoter.
This image was taken after 3 h of incubation using the *in-vitro* pollen germination system. The
areas surrounded by dashed lines are enlarged on the right side.
(B) A pollen tube from *kaku4-3* expressing *KAKU4-EYFP* under the control of *KAKU4* promoter.
This image was taken after 3.5 h of incubation using the *in-vitro* pollen germination system. The
pollen tube elongates toward the right of the panels.
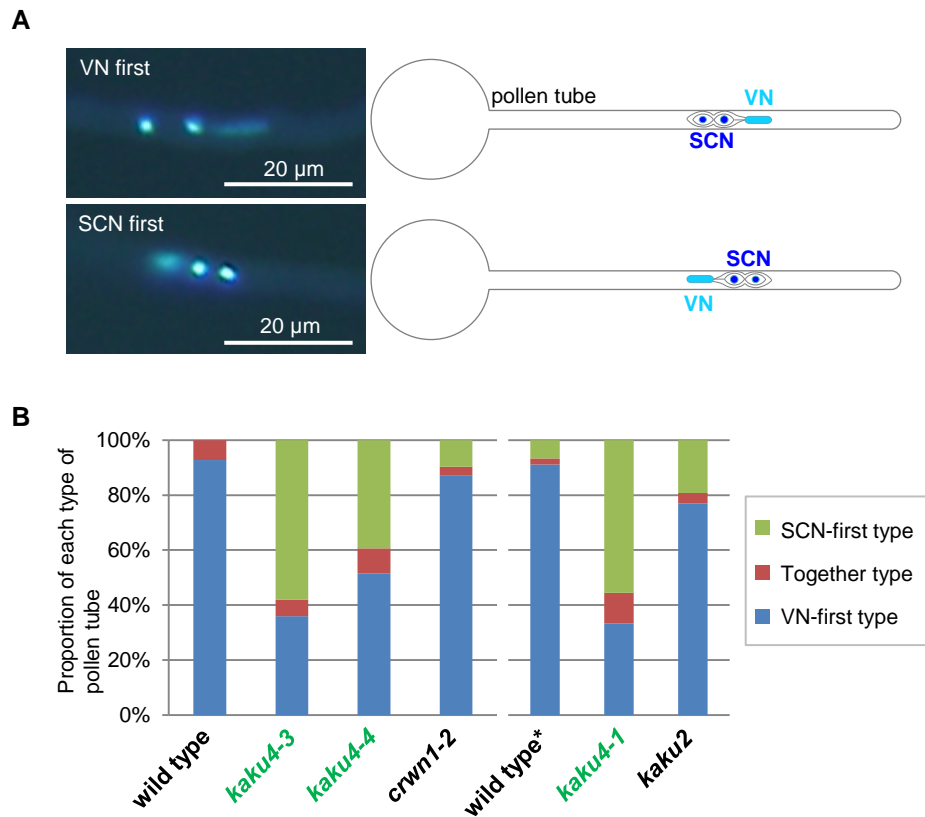Arrows indicate SCNs. DIC, differential interference contrast.

Fig. 5. Position of VN and SCN in pollen tubes of *kaku4*.
(A) (Left) Representative fluorescence images of nuclei in pollen tubes stained with Hoechst 33342. (Right) Diagrams of the photos showing the VN and two SCNs in pollen tubes. The diagrams are after Sprunck et al. 2014.
(B) Relative positions of VN and SCNs in wild-type, *kaku4* or *kaku2/crwn1* pollen tubes. Pollen grains were germinated on artificial medium at 22 ° C. The pollen tubes were fixed and stained with Hoechst 33342 after 3 h (for wild type, *kaku4-3*, *kaku4-4*, and *crwn1-2*) or 3.5 h (for wild type*, *kaku4-1* and *kaku2*) of incubation. The relative positions were categorized as VN-first type (VN is ahead of SCN), SCN-first type (SCNs are ahead of VN); and Together type (VN and SCN are close). In total, 55 (wild type), 50 (*kaku4-3*), 66 (*kaku4-4*), 31 (*crwn1-2*), 45 (wild type*), 18 (*kaku4-1*), and 26 (*kaku2 [crwn1]*) pollen tubes were tested. Wild type*, a transgenic plant expressing Nup50a-GFP (parental line of *kaku4-1* and *kaku2*).
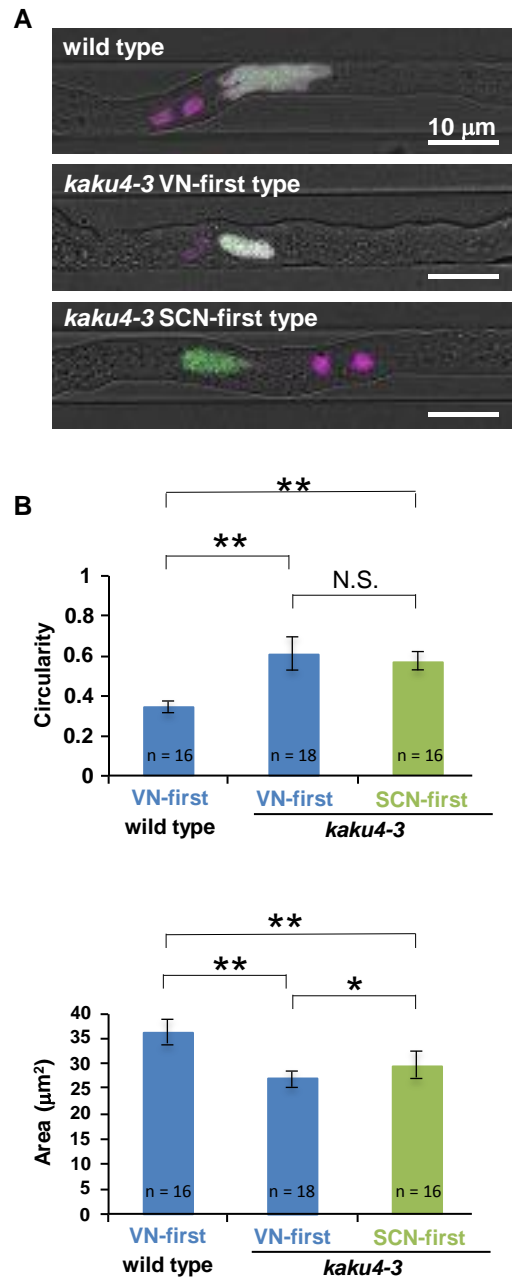
Fig. 6. Nuclear shape and size of VN in pollen tubes of *kaku4.*
(A) Representative fluorescence images of pollen tubes from the double nuclear marker line, in which the VNs were labeled with H2B-tdTomato (magenta) and NLS-Clover (green) and the SCNs were labeled with H2B-tdTomato (magenta). The pollen tubes were elongated in 10-µm-wide and 4-µm-depth channels of a polydimethylsiloxane microfluidic device and were analyzed after 1 h of incubation at 22 ºC.
(B) Circularity indices and areas of the VN in the VN-first-type pollen tubes of the wild-type plants and in the VN- and SCN-first-type pollen tubes of *kaku4-3* plants. Wild-type pollen tubes showed only VN-first-type positioning. The circularity index is defined as the equation $4\pi A/P^2$ (where A = area of nucleus and P = perimeter of nucleus) and indicates how closely each nucleus corresponds to a spherical shape (a perfect sphere has a circularity index of 1). Any deviation from a circular shape (e.g., elongated, lobulated, or spindle shaped) causes the index to decrease. Means ± standard errors for n = 16 (wild type), 18 (*kaku4-3* VN-first), or 16 (*kaku4-3* SCN-first). Asterisks indicate a significant difference (Student's *t* test, **$P < 0.001$, *$P < 0.005$).
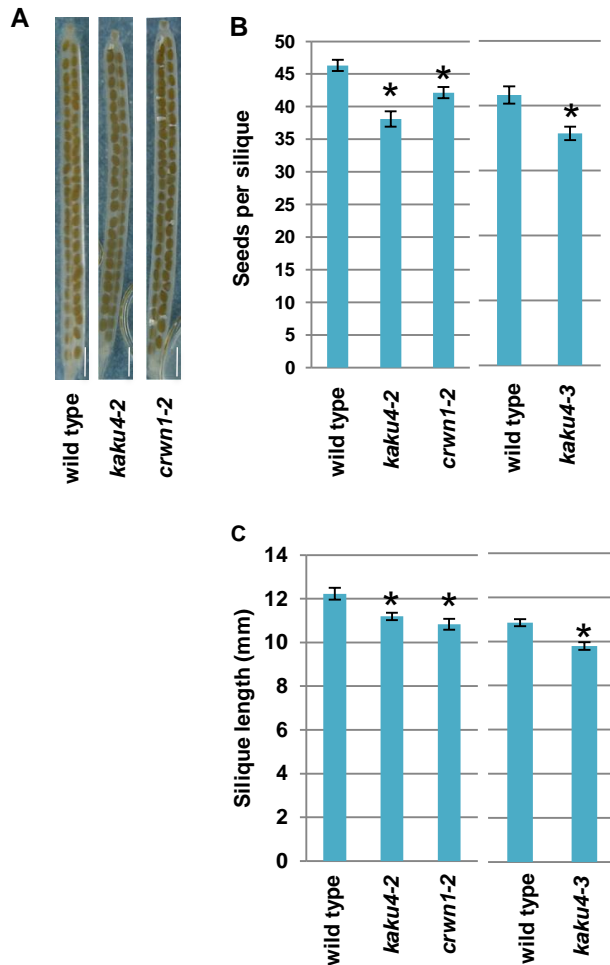
Fig. 7. Seed production in *kaku4*.
(A) Representative photographs of siliques of wild-type plant, *kaku4-2*, and *crwn1-2*. Bars = 1 mm.
(B) Number of seeds per silique from wild-type plant, *kaku4-2*, and *crwn1-2* (means ± standard errors for n = 60) (left) and the number of seeds per silique from wild-type plant and *kaku4-3* (means ± standard errors for n = 59 [wild-type] or 55 [*kaku4-3*]) (right).
(C) Length of the siliques from wild-type plant, *kaku4-2*, and *crwn1-2* (means ± standard errors for n = 23 [wild-type], 22 [*kaku4-2*], or 27 [*crwn1-2*]) (left) and length of the siliques from wild-type plant and *kaku4-3* (means ± standard errors for n = 62 [wild-type] or n = 55 [*kaku4-3*]) (right).
Asterisks indicate a significant difference from wild type (Student's *t* test, *P < 0.05).